

## A proposed model of the pressure field in a downburst

Z. Tang and L.Y. Lu\*

Key Laboratory for RC & PC Structures of Ministry of Education,  
Southeast University, Nanjing 210096, China

(Received January 25, 2011, Revised February 21, 2012, Accepted September 24, 2012)

**Abstract.** Pressure field and velocity profiles in a thunderstorm downburst are significantly different from that of an atmospheric boundary layer wind. A model of the pressure field in a downburst is presented in accordance with the experimental and numerical results. Large eddy simulation method is employed to investigate transient pressure field on impingement ground of a downburst. In addition, velocity profiles of the downburst are studied, and good agreement is achieved between the present results and the data obtained from empirical models.

**Keywords:** thunderstorm downburst; pressure field; large eddy simulation

---

### 1. Introduction

A downburst is a strong downdraft which induces an outburst of damaging winds on or near the ground. A downburst has significant pressure field and velocity distributions that are different from usual boundary layer winds. A downburst may occur in stormy or sunshiny days. It is very difficult to predict where and when it will occur. On 22<sup>nd</sup> of June, 2000, an airplane (flight Y7/B3479) crashed in Wu Han, China, which killed 42 people on board. The cause was a small downburst.

Researchers have proposed many methods of modeling certain aspects of downburst winds. Full-scale observations (Hjelmfelt 1988, Fujita 1990, Geerts 2001), give selected accounts of downbursts in different parts of the world. Moreover, some engineering usage models (Holmes and Oliver 2000, Wood *et al.* 2001) have been proposed. The small spatial and temporal scales of downbursts, however, make them extremely difficult to monitor. For this reason, several researchers have turned to physical and numerical simulation to further understand the damaging downbursts. Physical and numerical simulations (Sengupta 2008, Chay 2002, Mason *et al.* 2009, Tang and Lu 2010) have provided a better understanding of these phenomena.

This paper presents a model of the pressure field in a downburst in accordance with the experimental and numerical results. Large eddy simulation method is employed to investigate transient pressure field on impinging ground of a downburst. In addition, velocity profiles of the downburst are studied, and the results are compared with the data obtained from empirical models.

---

\*Corresponding author, Professor, E-mail: [llylu@seu.edu.cn](mailto:llylu@seu.edu.cn)

## 2. The proposed model

### 2.1 Mean pressure field

The pressure field in a downburst has been documented by Fujita (1985). On the central region of a downburst, a high-pressure ‘dome’ is formed when the downdraft approaches the ground. The relative magnitude of the pressure decrease depends on the jet exit velocity of the storm. Fujita speculated that these “rapid pressure changes could be as high as 2-3 hPa”, which may result in a significant increase in the load applied to large-span roofs beneath the downdraft.

The ground pressure coefficients are defined as  $C_p = (p - p_{\text{ref}}) / (0.5\rho \cdot V_{\text{jet}}^2)$ . On the impinging ground of a downburst, the pressure coefficients may be reasonably approximated by the following function:

$$C_p = e^{-\frac{1}{0.36} \left(\frac{r}{D}\right)^3} \quad (1)$$

Where,  $r$  is radial distance from jet centerline,  $D$  is jet diameter.

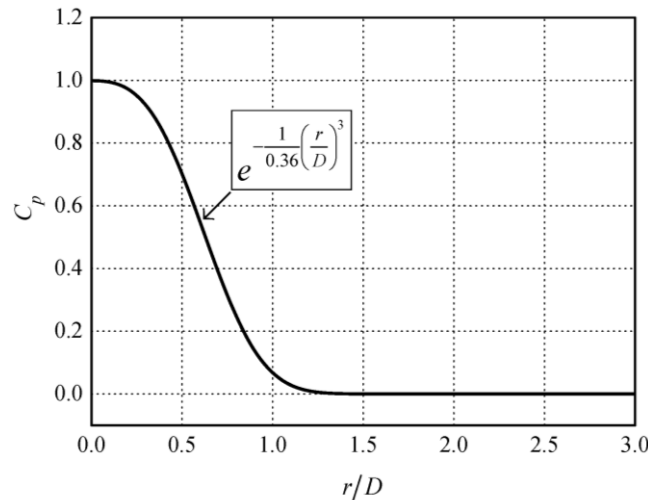


Fig. 1 Model profile of mean pressure field

Fig. 1 shows the pressure coefficients on the ground beneath the downdraft, given by Eq. (1) with representative value of  $D$ . The downburst produced a high-pressure region between  $0.0 \leq r/D \leq 0.2$  approximately equal to 1.0. As the downdraft was positioned further from  $r/D = 0.5$  the pressure coefficients showed a sharp decrease and quickly approached atmospheric pressure at  $r/D = 1.25$ . There is also good agreement between this profile and the experimental results (Sengupta 2008, Chay 2002), as shown in Fig. 2.

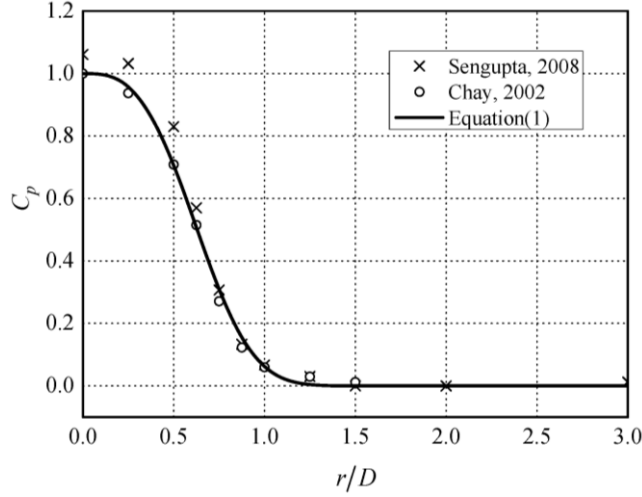


Fig. 2 Comparison of Eq. (1) with observed profiles by experiments

### 2.2 Transient pressure field

Significant variation of atmospheric pressure can be experienced within the flow field of a downburst. The varying pressure field of a downburst may have serious implications with respect to design loads on structures. Large eddy simulation method is employed to investigate transient pressure field on impingement ground of a downburst.

## 3. Numerical simulation of a downburst

### 3.1 Numerical modeling

The calculation method used here is the Large Eddy Simulation method. The governing equations employed for Large Eddy Simulation are obtained by filtering the time-dependent Navier-Stokes equations in either Fourier (wave-number) space or configuration (physical) space. The filtering process effectively filters out eddies whose scales are smaller than the filter width and grid spacing used in the computations. Thus the resulting equations govern the dynamics of large eddies.

Filtering the incompressible Navier-Stokes equations, one obtains

$$\frac{\partial \rho}{\partial t} + \frac{\partial}{\partial x_i} (\rho \bar{u}_i) = 0 \tag{2}$$

$$\frac{\partial}{\partial t} (\rho \bar{u}_i) + \frac{\partial}{\partial x_j} (\rho \bar{u}_i \bar{u}_j) = \frac{\partial}{\partial x_j} \left( \mu \frac{\partial \bar{u}_i}{\partial x_j} \right) - \frac{\partial \bar{p}}{\partial x_i} - \frac{\partial \tau_{ij}}{\partial x_j} \tag{3}$$

where  $\tau_{ij}$  is the subgrid-scale stress defined by

$$\tau_{ij} = \overline{\rho u_i u_j} - \rho \bar{u}_i \bar{u}_j \quad (4)$$

The subgrid-scale stresses resulting from the filtering operation are unknown, which thereby require modeling. The majority of subgrid-scale models in use today are eddy viscosity models of the following form:

$$\tau_{ij} - \frac{1}{3} \tau_{kk} \delta_{ij} = -2\mu_t \bar{S}_{ij} \quad (5)$$

where  $\mu_t$  is the subgrid-scale turbulent viscosity, and  $\bar{S}_{ij}$  is the rate-of-strain tensor for the resolved scale defined by

$$\bar{S}_{ij} = \frac{1}{2} \left( \frac{\partial \bar{u}_i}{\partial x_j} + \frac{\partial \bar{u}_j}{\partial x_i} \right) \quad (6)$$

The most basic of subgrid-scale models was proposed by Smagorinsky and further developed by Lilly . In the Smagorinsky-Lilly model (FLUENT 2005), the eddy viscosity is modeled by

$$\mu_t = \rho L_s^2 |\bar{S}| \quad (7)$$

where  $L_s$  is the mixing length for subgrid scales and  $|\bar{S}| \equiv \sqrt{2\bar{S}_{ij}\bar{S}_{ij}}$ .  $L_s$  is computed using

$$L_s = \min(\kappa d, C_s V^{1/3}) \quad (8)$$

where  $\kappa$  is the von Kármán constant,  $d$  is the distance to the closest wall,  $C_s$  is the Smagorinsky constant, and  $V$  is the volume of the computational cell.

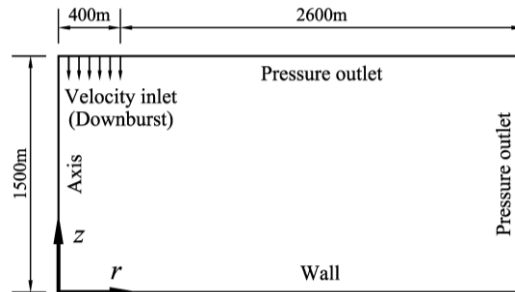


Fig. 3 Schematic diagram of computational domain

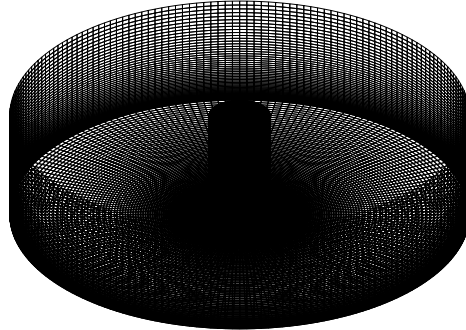


Fig. 4 Grid for simulation

The model was solved on a 3D (axisymmetric) non-uniform hexahedral grid. Fig. 3 shows the schematic diagram of the computational domain, where  $r$ -axis corresponds to the radial direction and  $z$ -axis corresponds to the axial direction, respectively. Fig. 4 shows a typical grid used for simulation (grid size: 1.2 million cells). A velocity inlet with constant velocity ( $V_{\text{jet}}=29$  m/s) and turbulence intensity (1.0%) was used. Kim and Hangan (2007) analysis of full-scale wind speed time histories supports the use of constant turbulence intensity. The impingement surface was a ‘no slip’ wall. Pressure outlets with a zero gauge pressure border the simulation domain. The simulations were run by using an unsteady solver, which was computationally more stable than a steady solver, until the flow achieved a steady state. The parallel computing system is built for the numerical wind tunnel, as shown in Fig. 5 and Table 1.

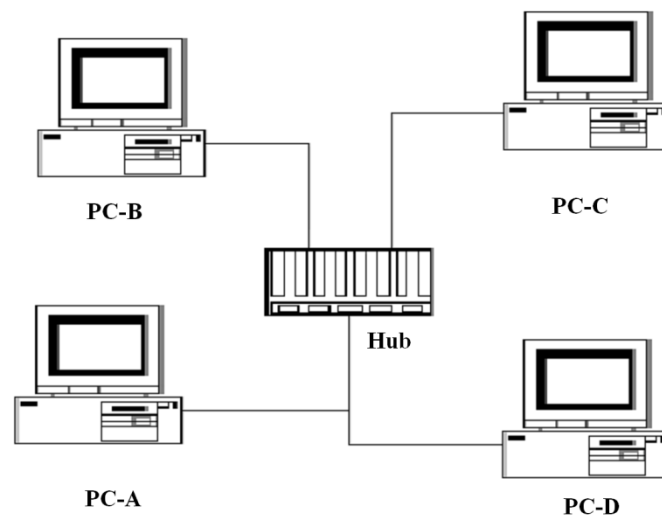


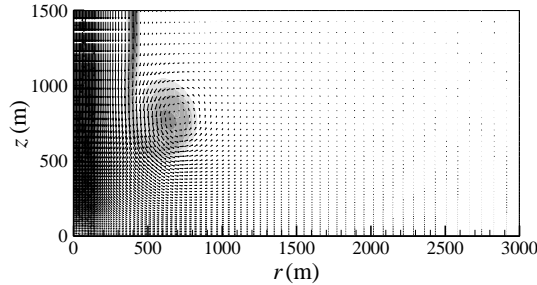
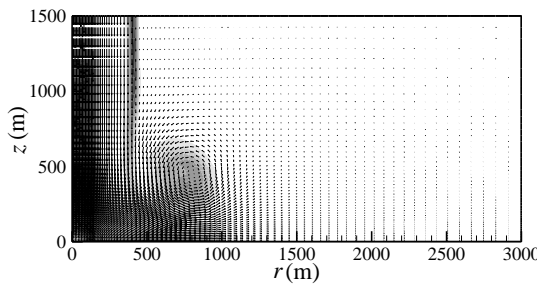
Fig. 5 The parallel computing system

Table 1 The hardware configuration of the parallel computing system

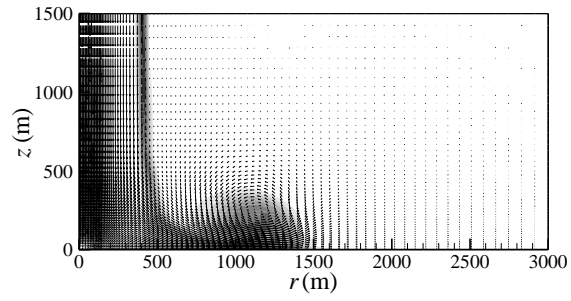
| No.             | PC-A               | PC-B | PC-C               | PC-D |
|-----------------|--------------------|------|--------------------|------|
| CPU             | Intel E8400 3.0GHz |      | Intel E8400 3.0GHz |      |
| Physical memory | 2G DDR2 1066       |      | 2G DDR2 800        |      |
| NIC             | 10/100Mbps         |      |                    |      |
| Switch          | D-Link 10/100Mbps  |      |                    |      |

### 3.2 Velocity field

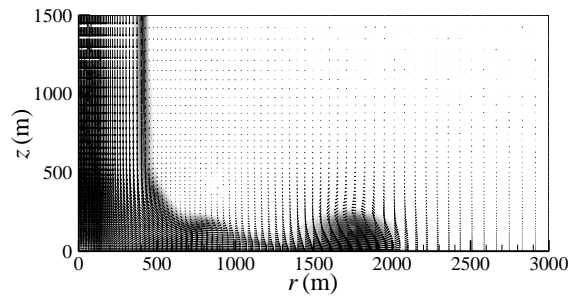
Large eddy simulations of a downburst were conducted in order to better understand the macro-scale dynamics of the flow. The results of these simulations show that as the jet flow is impulsively started ring vortices form due to the shear between the jet flow and the ambient still air. The ring vortices are then convected towards the impinging surface. Fig. 6 present snapshots of the flow field in terms of vorticity contours and velocity vectors for various non-dimensional time steps:  $T = t \cdot V_{\text{jet}} / D_{\text{jet}}$ . The six snapshots correspond to moments:  $T=2.850$ , 4.275, 5.700, 7.125, 8.550, and 9.975.

(1)  $T=2.850$ (2)  $T=4.275$ 

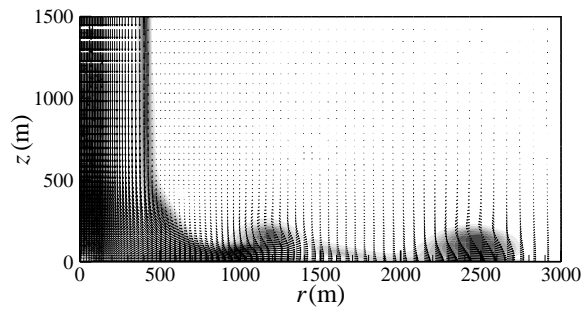
Continued



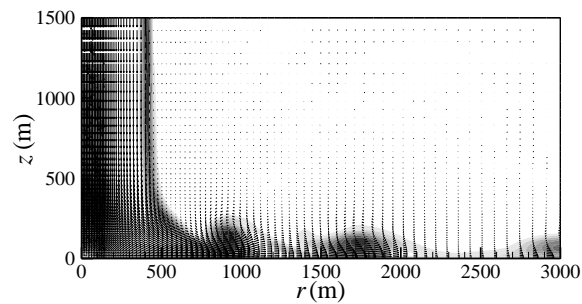
(3)  $T=5.700$



(4)  $T=7.125$



(5)  $T=8.550$



(6)  $T=9.975$

Fig. 6 Velocity vector and vorticity snapshots

Present numerical results are compared with semi-empirical models. The comparisons are based on a downburst diameter of 800m. Fig. 7 portrays the difference between a semi-empirical model proposed by Holmes (2000) and present numerical results at 10 m height. Fig. 8 shows the difference between a semi-empirical model proposed by Wood (2001) and present numerical results at  $r=800$  m. These figures suggest that semi-empirical models reproduce quite well the steady state radial flow field at 10 m height and  $r=800$  m. Meanwhile, the numerical time-dependent radial profiles show a pronounced variability of values during the time evolution of wind field. It can be seen that Large Eddy Simulation is able to predict the overall trend of velocity profile in a downburst with remarkable accuracy.

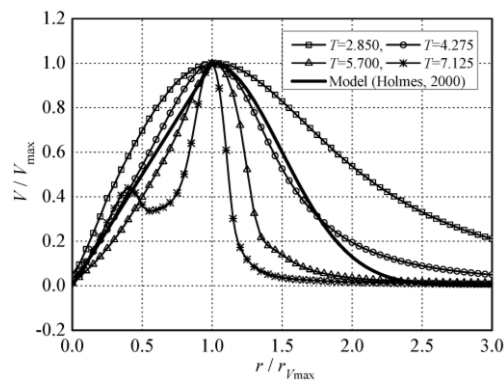


Fig. 7 Comparison of velocity profile at  $z=10$  m

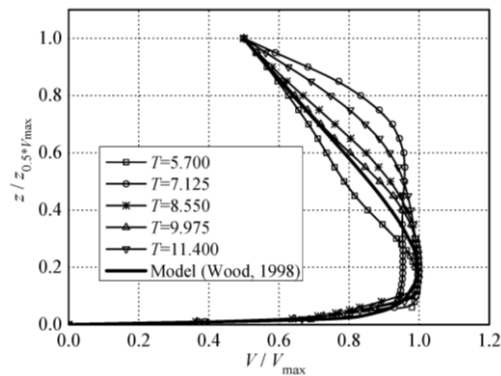


Fig. 8 Comparison of velocity profile at  $r=1.0D$

### 3.3 Pressure field

Fig. 9 shows the comparison among numerical transient pressure coefficients on the impinging ground due to different positions in a downburst. It can be seen that in a downburst, peak pressure coefficient value occurs when the first ring vortices arrives at the ground beneath the downdraft.

Subsequently, a series of peaks occur in response to the succeeding small ring vortices.

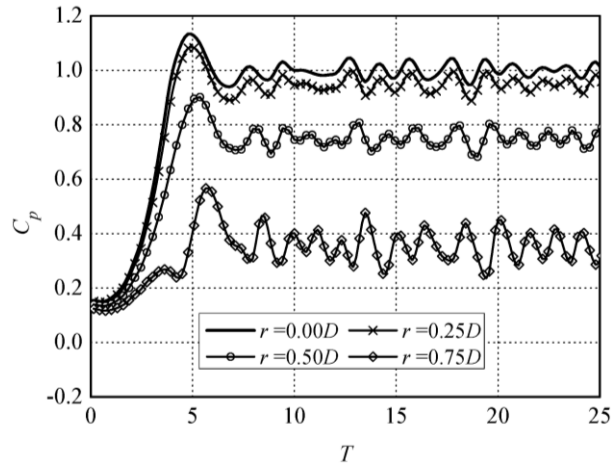


Fig. 9 Pressure coefficient on impingement ground

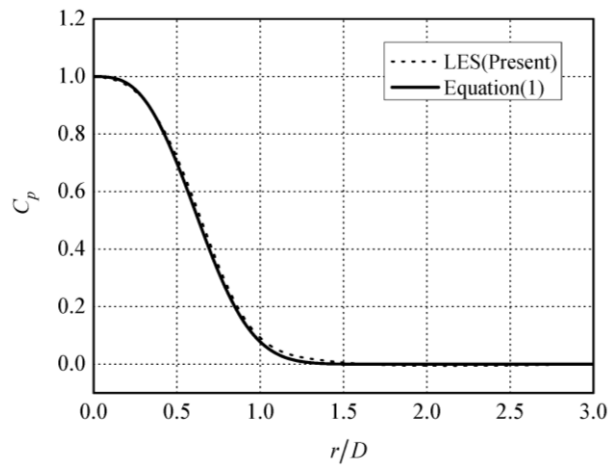


Fig. 10 Comparison of Eq. (1) with simulated profiles using LES

#### 4. Conclusions

This paper presents a model of the pressure field in a downburst in accordance with the experimental and numerical results. Large eddy simulation method is employed to investigate transient pressure field on impingement ground of a downburst. In addition, velocity profiles of the downburst are studied, and good agreement is achieved between the present results and the data obtained from empirical models.

## Acknowledgements

The work presented in this paper is supported by National Basic Research Program of China (No. 2007CB714200) and Specialized Research Fund for the Doctoral Program of Higher Education of China (No.20070286017).

## References

- Alahyari, A. and Longmire, E.K. (1995), "Dynamics of experimentally simulated microbursts", *AIAA J.*, **33**(11), 2128-2136.
- Bakke, P. (1957), "An experimental investigation of a wall jet", *J. Fluid Mech.*, **2**(5), 467-472.
- Chay, M.T. and Letchford, C.W. (2002), "Pressure distributions on a cube in a simulated thunderstorm downburst—Part A: stationary downburst observations", *J. Wind Eng. Ind. Aerod.*, **90**(7), 711-732.
- Choi, E.C.C. (2004), "Field measurement and experimental study of wind speed profile during thunderstorms", *J. Wind Eng. Ind. Aerod.*, **92**(3), 275-290.
- Darwish, M.M., El Damatty, A.A. and Hangan, H. (2010), "Dynamic characteristics of transmission line conductors and behaviour under turbulent downburst loading", *Wind Struct.*, **13**(4), 327-346.
- Droegemeier, K.K. and Wilhelmson, R.B. (1987), "Numerical simulation of thunderstorm outflow dynamics. Part I: outflow sensitivity experiments and turbulence dynamics", *J. Atmos. Sci.*, **44**(8), 1180-1210.
- Fluent. (2005), *FLUENT User's Guide, Release 6.2. Fluent Inc.*, Lebanon, New Hampshire.
- Fujita, T.T. (1985), *Downburst: Microburst and Macrobust*, University of Chicago Press, Chicago, IL, 122pp.
- Fujita, T.T. (1990), "Downburst: meteorological features and wind field characteristics", *J. Wind Eng. Ind. Aerod.*, **36**(1), 75-86.
- Geerts, B. (2001), "Estimating downdraft-related maximum surface wind speeds by means of proximity soundings in New South Wales, Australia", *Weather Forecast.*, **16**(4), 261-269.
- Holmes, J.D. and Oliver, S.E. (2000), "An empirical model of a downburst", *Eng. Struct.*, **22**(9), 1167-1172.
- Ivan, M. (1986), "A ring-vortex downburst model for flight simulations", *J. Aircraft*, **23**(3), 232-236.
- Kim, J. and Hangan, H. (2007), "Numerical simulations of impinging jets with application to downbursts", *J. Wind Eng. Ind. Aerod.*, **95**(4), 279-298.
- Kim, J., Hangan, H. and Ho, T.C.E. (2007), "Downburst versus boundary layer induced wind loads for tall buildings", *Wind Struct.*, **10**(5), 481-494.
- Letchford, C.W. and Chay, M.T. (2002), "Pressure distributions on a cube in a simulated thunderstorm downburst—Part B: moving downburst observations", *J. Wind Eng. Ind. Aerod.*, **90**(7), 711-732.
- Lin, W.E., Orf, L.G., Savory, E. and Novacco, C. (2007), "Proposed large-scale modelling of the transient features of a downburst outflow", *Wind Struct.*, **10**(4), 315-346.
- Hjelmfelt, M.R. (1988), "Structure and life cycle of microburst outflows observed in Colorado", *J. Appl. Meteorol.*, **27**(8), 900-927.
- Mason, M.S., Wood, G.S. and Fletcher, D.F. (2009), "Numerical simulation of downburst winds", *J. Wind Eng. Ind. Aerod.*, **97**(11), 523-539.
- Mason, M.S., Wood, G.S. and Fletcher, D.F. (2007), "Impinging jet simulation of stationary downburst flow over topography", *Wind Struct.*, **10**(5), 437-462.
- McConville, A.C. (2009), "The physical simulation of thunderstorm downbursts using an impinging jet", *Wind Struct.*, **12**(2), 133-149.
- Nicholls, M., Pielke, R. and Meroney, R. (1993), "Large eddy simulation of microburst winds flowing around a building", *J. Wind Eng. Ind. Aerod.*, **46-47**, 229-237.

- Orwig, K.D. and Schroeder, J.L. (2007), "Near-surface wind characteristics of extreme thunderstorm outflows", *J. Wind Eng. Ind. Aerod.*, **95**, 565-584.
- Selvam, R.P. and Holmes, J.D. (1992), "Numerical simulation of thunderstorm downdrafts", *J. Wind Eng. Ind. Aerod.*, **41-44**, 2817-2825.
- Sengupta, A. and Sarkar, P.P. (2008), "Experimental measurement and numerical simulation of an impinging jet with application to thunderstorm microburst winds", *J. Wind Eng. Ind. Aerod.*, **96**(3), 345-365.
- Shehata, A.Y. and El Damatty, A.A. (2007), "Behaviour of guyed transmission line structures under downburst wind loading", *Wind Struct.*, **10**(3), 249-268.
- Tang, Z. and Lu, L.Y. (2010), "A square cylinder and a hemisphere cylinder in downbursts", *Proceedings of the 2<sup>nd</sup> International Symposium on Advances in Urban Safety (SAUS 2010)*, Kobe, Japan.
- Vicroy, D.D. (1992), "Assessment of microburst models for downdraft estimation", *J. Aircraft*, **29**(6), 1043-8.
- Wood, G.S. and Kwok K.C.S. (1998), "An empirically derived estimate for the mean velocity profile of a thunderstorm downdraft", *Proceedings of the 7th AWES Workshop*, Auckland.
- Zhu, S.X. and Etkin, B. (1985), "Model of the wind field in a downburst", *J. Aircraft*, **22**(7), 595-601.

CC